Acta Geochim (2026) 45:99–110
https://doi.org/10.1007/s11631-025-00799-2

ORIGINAL ARTICLE

Fabrics of forsterite in CBa chondrite Sierra Gorda 013

Rong Li[1] · Wei Chen[1] · Chun-Hui Li[1]

Received: 26 August 2024 / Revised: 31 May 2025 / Accepted: 3 June 2025 / Published online: 14 June 2025

Abstract CB chondrite is a class of meteorite rich in metal composition, and its characteristics are obviously different from other chondrite groups. These meteorites are distinguished by their content of up to 60% to 70% FeNi metals and sulfides, in addition to their extreme lack of volatile and moderately volatile elements, less refractory inclusions, and almost no fine-grained matrix. Sierra Gorda 013 (SG 013) is a metal-rich chondritic meteorite of the CBa type. It has two different lithologies within SG 013: Lithology 1 and Lithology 2. Lithology 1 is an anomalous CBa chondrite containing chromite-pyroxene complex assemblage, whereas Lithology 2 is featured by recrystallization with small chondrules and contains much less iron nickel metal than Lithology 1. Although the two lithologies have essentially the same oxygen isotope composition, their structures are different from each other, suggesting that they probably underwent distinct formation and evolution processes from common precursors. In this study, the mineralogy of SG 013 chondrites is studied by means of petrographic observation, semi-quantitative analysis of chemical composition, fabric identification of minerals and integrated mineral phase analysis, while studying the mineralogy of SG 013, and the fabric characteristics of SG 013 are studied in detail. Different from previous studies, here we find that Lithology 1 of SG 013 contains non-porphyritic chondrules and metallic silicate globules, while Lithology 2 not only contains non-porphyritic chondrules and metallic-silicate globules, but also porphyritic chondrules. In this thesis, Electron backscatter diffraction (EBSD) analysis of magnesium olivine in metal-silicate globules and porphyritic chondrules in L2 of SG 013 shows that some magnesium olivine form under conditions of lower temperature and faster strain rate during uniaxial compression, where deformation of the olivine is dominated by dislocation glide. However, at higher temperatures and slower strain rates, the fabric of B-axis ([100]) is concentrated, indicating that the porphyritic chondrules may be dominated by the compaction of olivine particles, leading to dynamic recrystallization in the peripheral region or outer layer of the magnesium olivine crystal. New grains formed by dynamic recrystallization occur at the edges of residual grains and, their orientation is controlled by stress. It is found that the formation position of magnesium olivine in different chondrules of SG 013 from the inside out, with the gradual reduction of stress and the gradual increase of temperature, these local physicochemical changes reveal the complex thermal history and dynamic processes that chondrules undergo during their formation and evolution.

Keywords CBa chondrites · Sierra Gorda 013 · EBSD · Forsterite · Fabrics

1 Introduction

Carbonaceous chondrites are the most primitive meteorites that do not undergo metal-silicate differentiation and thus their texture and composition are more pristine than other solar system materials (Stewart et al. 2019; Meibom et al. 1999). CB chondrites are the most reduced sub-type of carbonaceous chondrites, therefore we might get insight into some extreme environments of the solar system from CB chondrites (Scott et al. 2007). CB typically contains large

✉ Rong Li
2406773196@qq.com

✉ Chun-Hui Li
lichunhui@cdut.edu.cn

[1] School of Earth and Planetary Sciences, Chengdu University of Technology, Chengdu 610059, China

metallic globules in 1.5–8 mm and silicate chondrules in centimeter size (Hewins et al. 2018). These metallic globules are not pure metal but have variable amounts of silicates and olivine. CB are characterized by high metal/silicate ratios, severe depletion in volatile elements, and absence of any fine-grained matrix material and hydrated silicate clasts (Oulton et al. 2016; Meibom et al. 2005). The absence of matrix material and hydrated silicates in CBa chondrites (e.g., SG 013) may indicate rapid thermal processing or the formation of chondrules through impact-generated steam jets (Metzler 2012).

Based on petrological and geochemical features including Fe-Ni metal abundance (40–80 vol%), chondrule size and structure, CB chondrites are further divided into coarse-grained CB_a and fine-grained CB_b subgroups (Weisberg et al. 2001). CBa chondrites contain approximately 60 vol% Fe-Ni metal, centimeter-sized magnesian skeletal olivine (SO), and cryptocrystalline (CC) non-porphyritic chondrule structures, but have no fine-grained matrix and refractory calcium-aluminum-rich inclusions (CAIs). CB_b chondrites have finer-grained chondrules and ~70 vol% Fe-Ni metal nodules, as well as some rare-type CAIs, porphyritic chondrules (Lofgren et al. 1989), and hydrated chondrule fragments. SO and CC chondrules from both subgroups are interpreted to have formed in impact-generated gas-melt jets at 4562.52±0.44 Ga (Krot et al. 2022b, a).

According to existence of chemical zoning, the metal globules in CB can be separated into two types (Rubin et al. 2003). Metal can directly condense from metal-rich vapors into liquid condensates (metal without compositional variations) and solid condensates (metal with compositional variations). Metal droplets may also form by splashing during the impact-generated gas-melt plume formation or prior to plume formation (Connolly et al. 1995). It is proposed that the silicates and metals in CB_a and CB_b are a consequence of impact but may form at different stages or locations within the vapor plume (Campbell et al. 2002). A proposed model suggests that CBa chondrites may originate from CBb precursor materials through high-temperature volatilization within a dense gas plume, followed by rapid condensation (Krot et al. 2022b, a). This is supported by the absence of hydrated silicates in CBa, consistent with brief thermal processing.

Sierra Gorda 013 (SG 013) is found in the Chilean desert in 2018 and is classified as CBa (Ivanova et al. 2022). The weathering grade of SG 013 is W3, which means that it is affected by low-to intermediate weathering processes (Wlotzka 1993). One example is that oxidized metallic and gypsum around the silicate minerals. Although lithological clasts from SG 013 have two distinct textures, their oxygen isotope compositions are identical. This demonstrates that the lithological clasts were derived from the same precursor but took different evolutionary paths (Lorenz et al. 2023). Despite previous reports of porphyritic chondrules in CB_a materials (Ivanova et al. 2023), their presence in SG 013 remains unresolved, raising questions about their formation mechanism in impact plumes. In order to provide more constraints on the petrogenesis of SG 013, combined with mineralogical and petrological investigations, here we present the results from electron backscatter diffraction (EBSD) analysis of forsterite in SG 013, which might reveal more details of the processes of chondrules underwent.

2 Sample and methodology

The SG 013 meteorite sample consists of 8 fragments with a total mass of 804 g. Its surface exhibits a fusion crust partially covered by brown weathering products (Wlotzka et al. 1993). A thin section (~0.6 mm thickness) was prepared for analysis.

Tescan Integrated Mineral Analyzer (TIMA) measurements were conducted at the Key Laboratory of Orogenic Belts and Crustal Evolution, Peking University. The TIMA system (Tescan Mira Schottky field emission SEM) integrates four silicon drift EDS detectors arranged at 90° intervals. High-resolution backscattered electron (BSE) imaging was performed at 25 kV with a spot size of ~110 nm, working distance of 15 mm, and scan area of 1500 μm. Distinct mineral phases were identified through X-ray spectral matching against standard mineral definition databases, with automated calculation of volumetric and mass proportions.

Mechanical polishing was performed using diamond suspension and alumina slurry to remove surface deformation layers (nanometer-scale artifacts from initial grinding). This process ensures that backscattered electron signals accurately reflect intrinsic crystallographic features.

The EBSD analysis in this study was conducted at the Laboratory for Astrochemistry and Planetary Sciences, Purple Mountain Observatory, Chinese Academy of Sciences, using a Hitachi S-3400N SEM equipped with an Oxford Instruments Nordlys Nano EBSD detector. Aztec data acquisition software and HKL/Channel-5 software were employed for data collection and processing. For optimal Kikuchi pattern acquisition: (1) Low-magnification regions were scanned in fast mode to identify target areas; (2) High-resolution slow scanning (with optimized dwell time) minimized background noise; (3) Kikuchi patterns were indexed by matching against standard mineral databases through iterative refinement (automatic band detection followed by manual adjustment of band positions); (4) Crystal orientations and phase identifications were validated through cross-comparison with pole figures generated using the Mambo program (HKL-Oxford Instruments).

3 Results

The SG 013 is primarily composed of chondrules and their fragments, along with Fe-Ni metal. Silicates are predominantly present in the form of large barred olivine and small porphyritic chondrules. As shown in Fig. 1, the silicate minerals mainly include olivine (~5.9 vol%) and pyroxene (~17.7 vol%). The opaque minerals (~76.4 vol%) are primarily composed of Fe-Ni metal. All olivine are forsterite (Fo 95.1 ± 0.6). Figure a is the BSE diagram of SG 013, and Figure b is the TIMA phase diagram of SG 013, including metallic iron, enstatite, olivine and some secondary minerals such as calcite, magnetite/hematite, gypsum, etc.

3.1 Mineralogy of the SG 013 chondrules

In the SG 013, the boundaries of most chondrules are not well-defined but fragmented. The size of chondrules varies from 0.5 mm to 2.4 mm. 10 chondrules were investigated and can be classified into five different types of chondrules, including 3 porphyritic olivine pyroxene (POP) chondrules, 2 non-porphyritic chondrules, and 5 metal-silicate globules. Nearly all the chondrules are rich in magnesium, but they do not have other characters including residual grains, coarse igneous rims and fine-grained matrix as edges. Table 1 shows the structure classification of chondrules. The chemical compositions of Olivine, Enstatite, and Diopside in L2 are shown in Tables 2, 3, and 4, respectively.

Porphyritic Olivine Pyroxene (POP) Chondrules: The diameters of the 3 POP chondrule-sized grains are 0.4 mm, 0.5 mm, 0.2 mm, and they are all spherical shape. As shown in Fig. 2, two larger POP chondrules have clear boundaries and are surrounded by forsterite, pyroxene phenocrysts, and opaque minerals (Fe-Ni metal). BSE images of silicate mineral grains show significant brightness differences between a dark gray core (lower MgO and higher FeO content) and a light gray rim (with lower FeO and higher MgO content). The silicate minerals are fractured and filled by opaque metallic minerals. Fine-grained olivine grains show reduction rim, exhibiting banding characteristics. Additionally, irregular-shaped pores between fine olivine grains can also be observed. There are structural differences between the core and rim of olivine grains: (1) content and size of metals in the core are smaller, otherwisely larger in the rim; (2) the core of coarse-grained olivine has less pores compared with the grains in the rim. As shown in Tables 2 and 3, the olivine phenocrysts (MgO=54.1 wt%) are more magnesium-rich compared to enstatite (MgO=36.7 wt%). Enstatites contain exsolutions of metal sulfides, and enstatites becomes more magnesium-rich (darker) towards the exsolutions. According to the composition of olivine in the three porphyritic chondrules in the Table 5, it is found that the composition is relatively uniform and the heat treatment degree is similar.

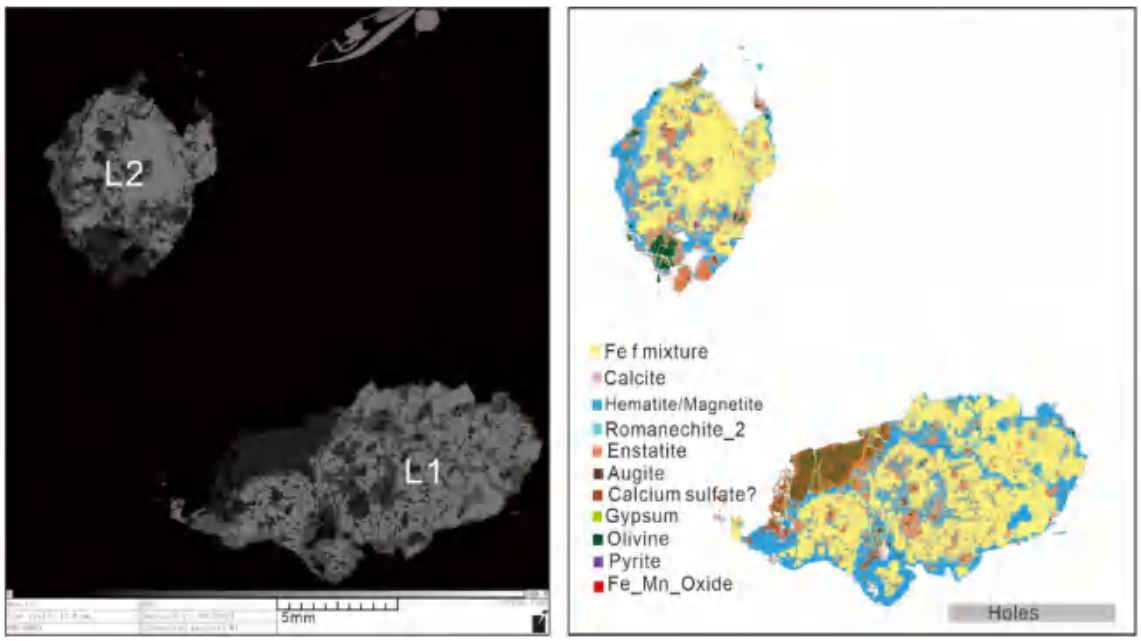

Fig. 1 BSE diagram of Sierra Gorda 013 meteorite thin slices. *Note*: Test instrument: Tescan Integrated Mineral Analyzer (TIMA); Test conditions: acceleration voltage 25 kV, spot size 110 nm, working distance 15 mm; Testing unit: Key Laboratory of Orogenic Belts and Crustal Evolution, School of Earth and Space Sciences, Peking University; Test time: August 2023

Table 1 Structure classification of chondrules (Gooding and Keil 1981)

Type	For short	Texture		For short	1/10 ≤ Ol/Px ≤ 10/1 (Volume ratio, same below)
I type (poor FeO, olivine Fo > 90)	IAB, between IA and IB	Porphyritic chondrules	Porphyritic Olivine Pyroxene chondrules	POP	L2-POP-3 (0.190)
					L2-POP-2 (0.123)
					L2-POP-4 (0.100)
	IA, ol > 80% olivine/(olivine + pyroxene) Volume ratio	Non-porphyritic chondrules	Barred Olivine chondrules	BO	L1-BO-1 (1.157)
	IB, px > 80% olivine/(olivine + pyroxene) Volume ratio		Cryptocrystalline chondrules	CC	L2-Mg-CC-1
			Metal-Silicate Globules	MSG	L1-MSG-1
					L1-MSG-2
					L1-MSG-3
					L1-MSG-4
					L2-MSG-1

Table 2 Chemical composition of olivine in SG-L2 (wt%) (Fo value is 95.1 ± 0.6) (Energy spectrum analysis)

N	MgO	MnO	FeO	SiO_2	Cr_2O_3	Total	Fo
1	54.0	n.d.	3.0	42.9	n.d.	100.0	94.7
2	54.3	0.1	2.7	42.7	0.1	100.0	95.3
3	54.4	n.d.	3.0	42.7	n.d.	100.0	94.8
4	53.4	n.d.	2.8	42.1	1.7	100.0	95.0
5	54.3	n.d.	2.7	43.0	n.d.	100.0	95.3
6	54.1	n.d.	2.8	43.1	n.d.	100.0	95.1
7	54.2	n.d.	3.0	42.8	n.d.	100.0	94.8
8	54.2	n.d.	3.1	42.7	n.d.	100.0	94.6
9	54.4	n.d.	2.6	43.0	n.d.	100.0	95.4
10	54.6	n.d.	2.5	42.9	n.d.	100.0	95.6

N indicates the number of detection points

Table 3 Enstatite components of SG-L2 (wt%) (Mg# value 94.4 ± 0.48) (Energy spectrum analysis)

N	MgO	Al_2O_3	TiO_2	FeO	CaO	SiO_2	Cr_2O_3	$Mg^{\#}$	Total
1	36.5	1.1	0.3	2.0	1.0	58.1	1.0	94.8	100.0
2	36.6	0.8	n.d.	2.1	0.8	58.4	0.7	94.6	100.0
3	36.3	1.1	n.d.	2.2	0.9	58.6	0.9	94.3	100.0
4	36.5	0.9	n.d.	2.2	1.0	58.7	0.6	94.3	100.0
5	36.2	0.9	n.d.	2.2	1.2	58.5	0.9	94.3	100.0
6	36.1	0.8	n.d.	2.1	1.0	59.1	0.9	94.5	100.0
7	36.7	0.8	n.d.	2.2	1.0	58.5	0.7	94.3	100.0
8	36.5	0.8	n.d.	2.1	1.0	58.8	0.7	94.6	100.0
9	36.1	1.1	n.d.	2.3	0.9	58.3	0.9	94.0	100.0
10	36.0	0.9	0.3	2.0	1.1	58.4	0.9	94.7	100.0

N indicates the number of detection points

Barred Olivine (BO) Chondrule: we only observed one BO chondrule which appears as a fragment. As shown in Fig. 3, this chondrule is primarily composed of forsterite, displaying a comb-like structure with a set of parallel and stretched olivine phenocrysts. Chondrule is surrounded by a ring of smaller

Table 4 Diopside chemical composition (wt%) in SG-L2 (Mg# value 91.7 ± 5.9)

N	MgO	Al_2O_3	TiO_2	FeO	CaO	SiO_2	Cr_2O_3	$Mg^{\#}$	Total
1	18.6	1.5	0.5	1.5	22.2	54.8	0.9	92.5	100.0
2	18.8	1.5	0.7	1.8	22.0	54.4	0.8	91.3	100.0
3	18.6	1.4	0.7	3.5	21.5	53.5	0.8	84.2	100.0
4	19.1	1.4	0.5	2.4	21.7	54.0	0.9	88.8	100.0
5	19.2	1.4	0.5	1.8	22.1	54.2	0.8	91.4	100.0
6	17.3	4.1	0.5	0.9	22.4	53.8	1.0	95.1	100.0
7	18.8	1.6	0.7	1.1	22.0	54.7	1.1	94.5	100.0
8	18.4	2.0	0.7	1.3	22.5	53.5	1.7	93.4	100.0
9	18.5	1.7	0.8	2.0	21.8	54.2	1.0	92.7	100.0
10	20.5	1.1	0.3	1.2	20.7	55.5	0.7	94.5	100.0
11	18.7	1.9	0.7	1.8	21.9	54.0	1.0	91.2	100.0
12	18.7	1.4	0.5	1.8	22.5	54.2	0.8	91.2	100.0

N indicates the number of detectionpoints

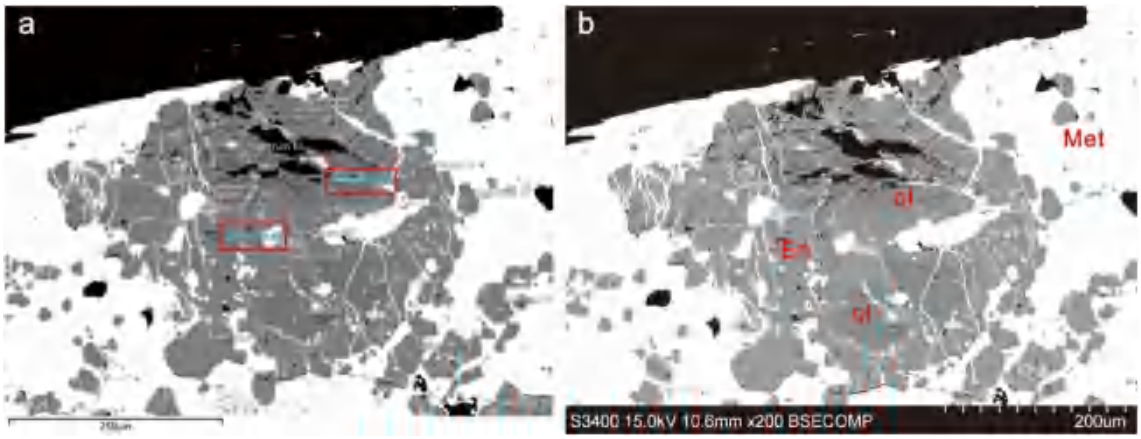

Fig. 2 SG 013 large POP porphyritic olivine pyroxene chondrules in meteorite

Table 5 Composition of magnesium olivine from porphyritic chondrules in the SG 013 chondrite (Spectroscopic analysis)

Sort	Spectrum	n	Mg	Si	Fe
L2-POP-4	Spectrum 48	ol1	54.3	42.9	2.8
	Spectrum 50	ol2	54.3	43.1	2.6
	Spectrum 51	ol3	54.2	43.0	2.9
	Spectrum 59	ol4	54.1	42.9	3.0
	Average	-	54.2	42.8	2.8
L2-POP-3	Spectrum 62	ol1	54.1	43.0	2.9
	Spectrum 63	ol2	54.2	43.0	2.9
	Spectrum 67	ol3	54.5	42.9	2.6
	Spectrum 70	ol4	54.4	43.0	2.6
	Average	-	54.3	43.0	2.8
L2-POP-2	Spectrum 07	ol1	54.6	42.9	2.5
	Spectrum 41	ol2	54.3	43.2	2.5
	Spectrum 42	ol3	54.5	43.3	2.2
	Average	-	54.5	43.1	2.4

n indicates the number of detection points.

olivine grains. The space between the barred olivine is mainly filled with feldspar and pyroxene. (Tables 6 and 7)

Magnesian Cryptocrystalline (Mg-CC) Chondrule: The size of the magnesian cryptocrystalline chondrules is 1343 μm and the area is 1416301 μm^2. The one Mg-CC chondrule has a distinguishable spherical shape. As shown in Fig. 4, magnesian cryptocrystalline chondrule is mainly composed of enstatite. In the BSE image, metal veins are observed along fractures within the chondrule (Fig. 4).

Metal-Silicate Globules: Five metal-silicate globules were observed by us. It is a metal-silicate substance composed of Fe-Ni metal, forsterite and enstatite. Metal-silicate globules are replaced by iron and nickel-metal hydride oxides at the grain contact. (Figs. 5, 6, and 7)

Fig. 3 Analysis of L1-BO chondrules and their mineral composition in SG 013 meteorite *Note*: Test instrument: Tescan Integrated Mineral Analyzer (TIMA); Test conditions: acceleration voltage 25 kV, spot size 110 nm, working distance 15 mm; Testing unit: Key Laboratory of Orogenic Belts and Crustal Evolution, School of Earth and Space Sciences, Peking University; Test time: August 2023

Table 6 Pyroxene composition in the chondrites of meteorite SG 013 L2-POP-3 (Spectroscopic analysis)

	n	Mg	Si	Fe	Al	Ca
Spectrum 64	En1	36.4	58.3	2.4	1.1	0.8
Spectrum 65	En2	36.7	58.7	2.0	1.0	0.9
Spectrum 66	En3	36.2	59.0	2.1	0.8	1.1
Spectrum 71	En4	36.1	58.4	2.4	1.0	1.3
Spectrum 72	En5	36.2	58.1	2.7	1.0	1.1
Spectrum 73	En6	36.3	58.4	2.6	0.8	1.2
Average		36.3	58.5	2.4	1.0	0.9

n indicates the number of detection points

Table 7 The size and area of chondrules

Chondrule type	Size (μm)	Area (μm^2)
L2-MSG-1	1353	1,438,713
L2-POP-2	1149	1,036,526
L2-POP-3	861	582,272
L2-POP-4	867	590,988

3.2 Fabrics of forsterites in SG 013-L2- POP and metal-silicate globules

In order to reveal the deformation history SG 013 underwent, we used EBSD to investigate the fabrics of forsterite crystals. As shown in (Fig. 8), localized enlarged surface scans were performed on forsterites and all images were obtained within 24–48 minutes. Warm colors indicate high-density pole figures, whereas cool colors represent low-density pole figures.

The study revealed a concentrated distribution of crystalline orientation projection points at location 1, forming a distinct pole density, with a well-developed point pole density, implying uniaxial compression deformation. The development of the preferred orientation at this time is mainly due to the combination of intracrystalline sliding and grain rotation mechanisms. In contrast, the crystalline orientation projection points at locations 3, 4, and 2 exhibit a Type I cross girdle, forming a ring-like pole density.

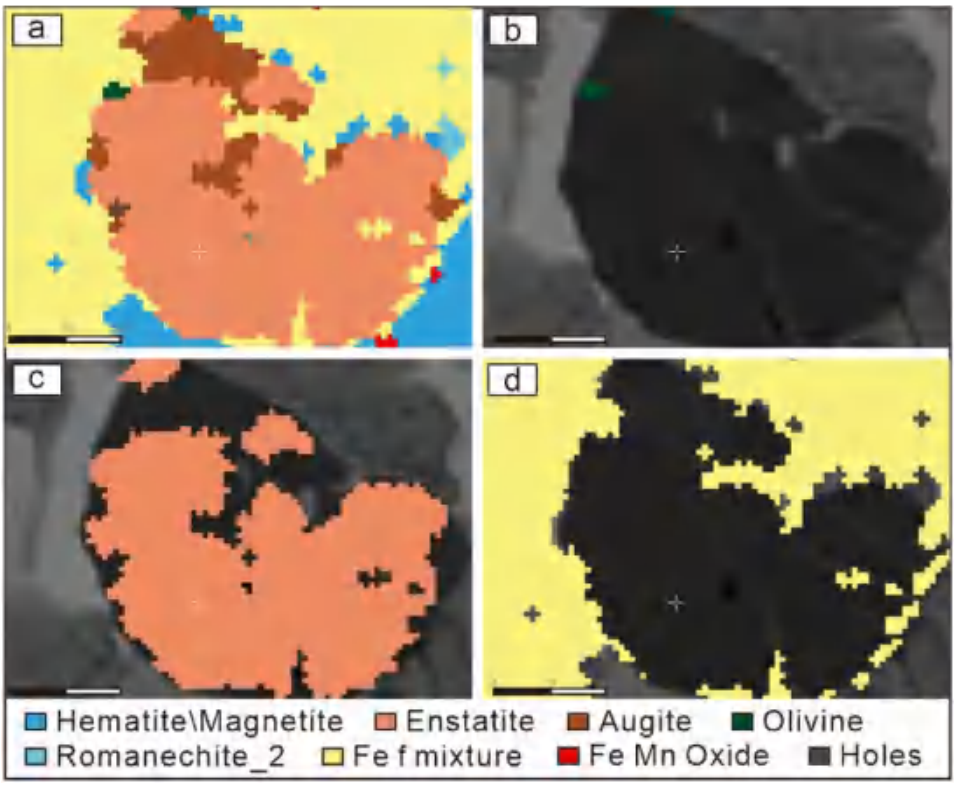

Fig. 4 Analysis of L2-magnesian CC chondrules and their mineral composition in Sierra Gorda 013 meteorite

4 Discussion

4.1 Comparison about the chondrules and globules

4.1.1 Compositional and mineralogical homogenization

The mineral composition of SG 013, as a carbonaceous chondrite of CBa type, shows a certain homogeneity. For example, the Barred Olivine (BO) are mainly forsterite and show a comb-like structure, indicating a consistent internal mineral composition despite being fragmented. The Magnesian Cryptocrystalline (Mg-CC) were mainly composed of enstatite and showed a high concentration of MgO.

In addition, the metal-silicate globules contain Fe-Ni metal, enstatite and pyroxene particles (Lofgren et al. 1986; Weyrauch et al. 2018), and the distribution and interrelations of these particles in the meteorite reflect a certain degree of mineralogical homogeneity, especially the chemical reaction between the metal and the silicate to form iron and nickel metal hydroxide. This suggests that under high temperature conditions, the melting and recrystallization processes that can occur between different minerals resulting in the mixing of different mineral.

SG 013 is lack of fine-grained matrix materials and its abundance of volatile elements. CB class carbonaceous chondrites generally contain a high proportion of metals/silicates and are heavily depleted in volatile elements, which means that during their formation, the minerals and metals likely underwent extensive melting and mixing, resulting in compositional and mineralogical homogenization (Kallemeyn et al. 1978). For SG 013, based on the idea that it originated from impact-generated steam jets, the various minerals and metals inside it may have undergone similar high temperature and high pressure environments at the same source, eventually forming a relatively uniform mineral assemblage (krot et al. 2023).

However, it is worth noting that although there is some homogeneity overall, different types of chondrules and other components still show different genetic backgrounds and microstructure characteristics, suggesting that even within homogenous materials, different formation stages and locations may lead to differences in mineral compositions and structures. For example, the differences between the CBa subgroup and the CBb subgroup may be due to their formation processes at different stages of the impact jet (Bollard et al. 2015). Therefore, the mineralogy and composition of SG 013 meteorite reflect in general homogeneity on a large scale and local diversity on a micro level.

4.1.2 Stress analysis

Stress not only affects the initial formation of chondrules, but also determines the structure and texture characteristics of the minerals inside them. Uniaxial compression results in an extremely dense distribution of points (Fig. 8), which reflects rapid cooling and transient deformation.

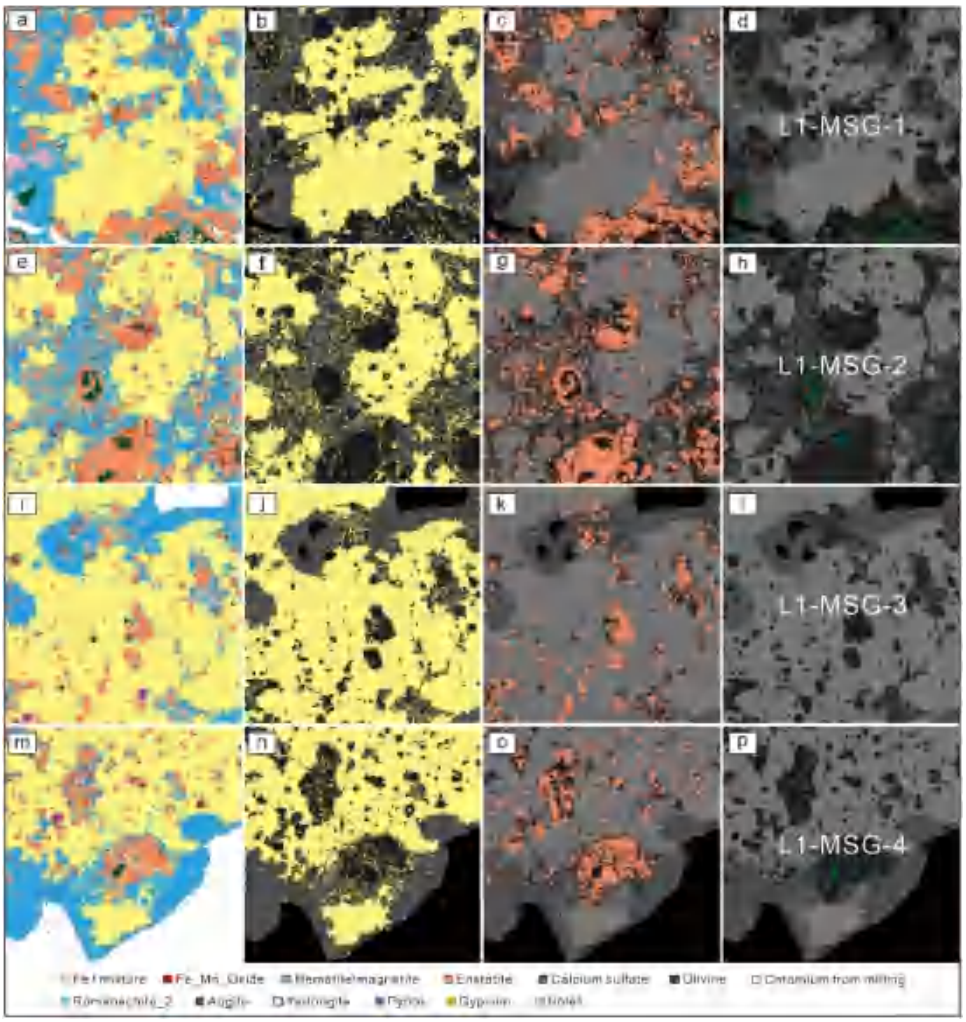

Fig. 5 Analysis of L1- metal-silicate chondrules and their mineral composition in Sierra Gorda 013 meteorite

Recrystallization, which forms an extremely dense girdle, reveals long-term, slow deformation and interactions between minerals as the molten material cools and crystallizes (Fig. 8). This occurs under conditions of slower strain rates. As the strain rate decreases, the half-opening angle of the ring continues to increase until it reaches 40°. The size of the half-opening angle of the ring also indicates the intensity of strain. According to Price (1985), circular ring patterns generally appear in rocks subjected to axisymmetric compressive or tensile deformation. Small circular rings produced by axisymmetric compression have half-opening angles around 25° to 40°, while those formed by axisymmetric tensile deformation have larger half-opening angles, ranging from 50° to 60° or 70° to 80°. Therefore, the ring-like pole density observed here is generated by axisymmetric compression. The development of the preferred orientation at this time is mainly attributed to recrystallization mechanisms. The development of preferred orientation during recrystallization depends on both the deformation circumstances and the characteristics of the deformed particles beforehand, specifically their size, shape, and orientation. Observations by Tullis et al. (1987) indicate that recrystallized particles are mostly oriented at an angle of 20° to 40° with respect to the main crystal.

4.2 Origins of SG 013

The zones of olivine-pyroxene is consistent with the high-temperature equilibrium of solar gas, as olivine condenses at higher temperatures than pyroxene. Metal veins fill the cracks or pores of the porphyritic chondrules, indicating traces of volatile activity during the high-temperature process of the metal jet flow. The high metal abundance and low FeO content in silicates suggest a reducing environment, although less reducing compared to enstatite chondrules. Due to reduction, a small amount of metal particles is distributed within the olivine of the chondrules. Summarizing the impact metamorphic effects on the SG 013 meteorite, it can be inferred that olivine underwent initial melting

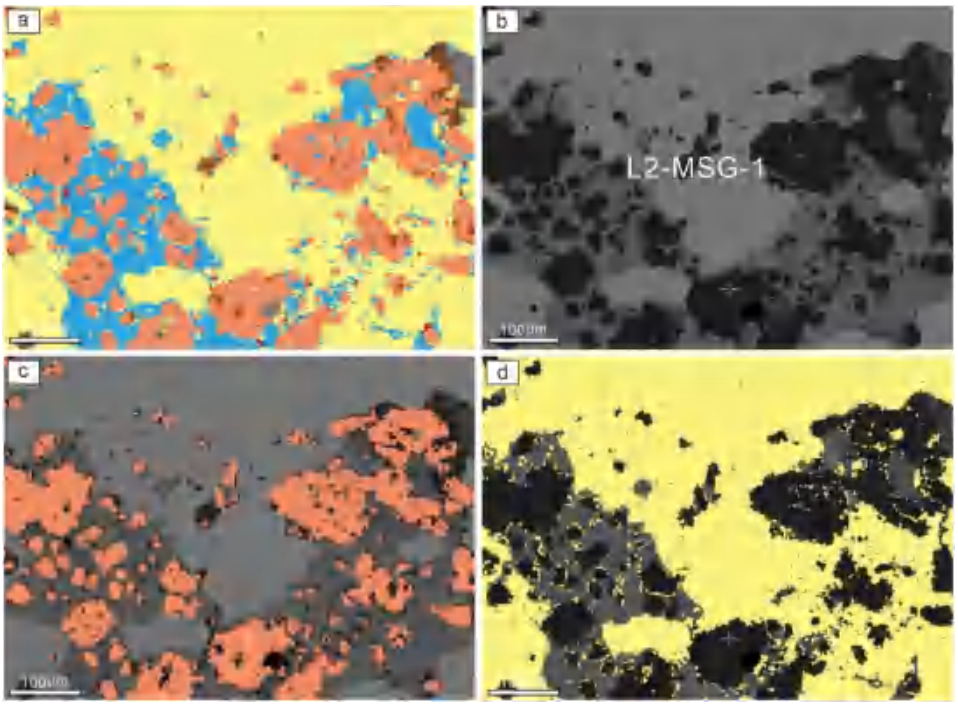

Fig. 6 Analysis of L2- metal-silicate chondrules and their mineral composition in Sierra Gorda 013 meteorite

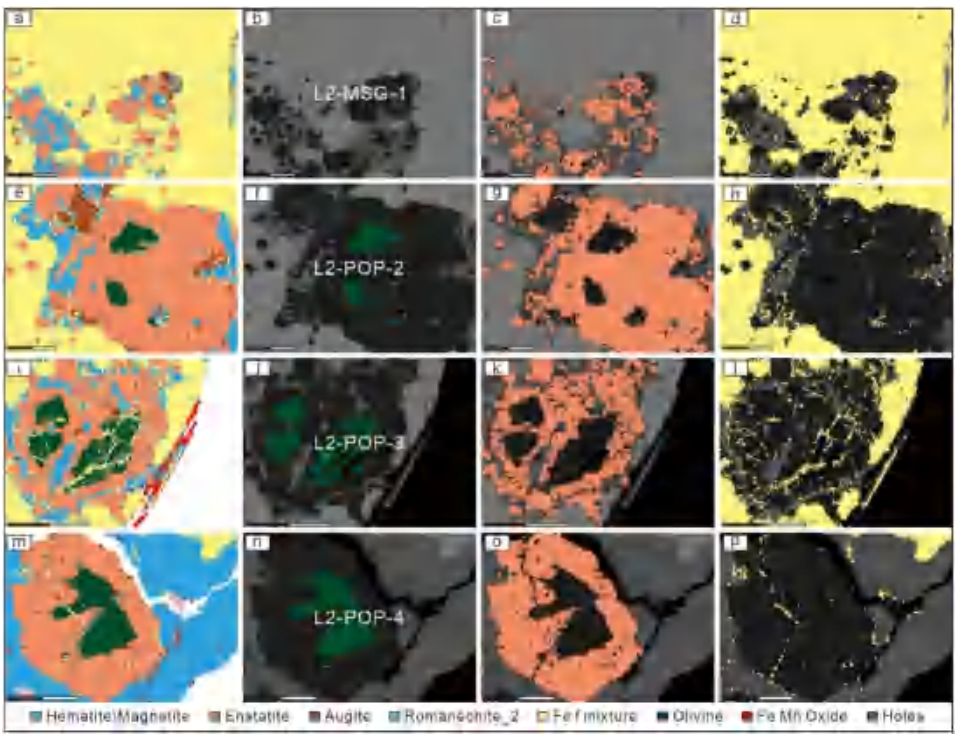

Fig. 7 Analysis of L2 chondrules and their mineral composition in Sierra Gorda 013 meteorite

(melting filling between particles) to pore formation, finally resulting in reduced metal filling (see Fig. 5).

Plastic flow of metal can explain the formation of metal nodules and the appearance of bands in the fractured matrix. Angular fragments in Sierra Gorda consist of fine-grained coexistence of magnesium-rich low-calcium pyroxene and Fe-Ni metal. The lack of matrix may indicate rapid thermal accretion, as suggested by Metzler (2012). Low-calcium pyroxene has extensively replaced magnesium olivine (in BSE images, magnesium olivine appears slightly darker than low-calcium pyroxene) (see Fig. 6).

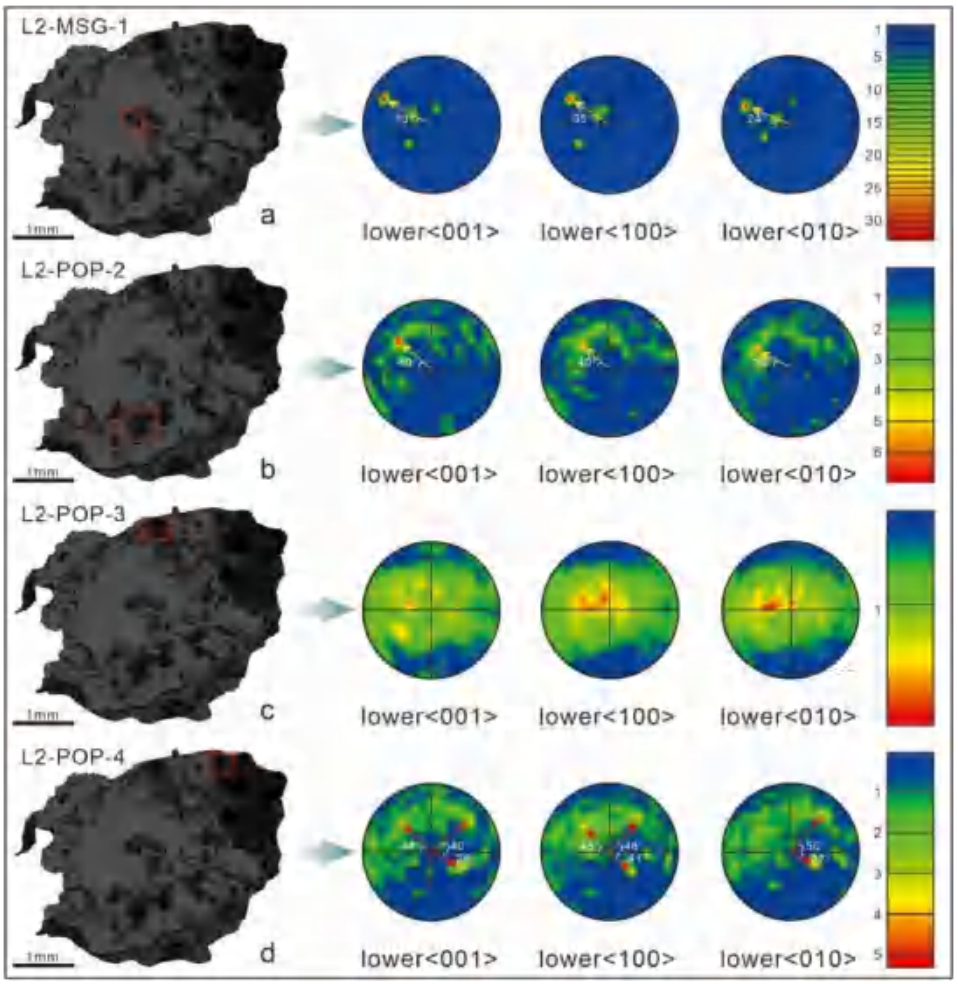

Fig. 8 EBSD fabric analysis of chondrules in Sierra Gorda 013 meteorite

The Metal-Silicate globule chondrules are formed by the co-melting of iron and silicate, where silicate serves as a flux, aiding in lowering the melting point and enhancing melting efficiency. Simultaneously, it helps control the viscosity and fluidity of the melt. In this process, the mixture of iron and silicate is heated to high temperatures and gradually cooled (see Fig. 8). The large plume volume and the random mixing of materials into the plume during the impact process, these minerals are dispersed and processed in the impact plume, and are systematically captured by the metal spheres through stress driving.

The evolutionary model of impact plumes suggests that, due to the interaction of the expanding plumes in the gaseous protoplanetary disk (Hasegawa et al. 2016; Carter and Stewart 2020; Sanders et al. 2005), the material from disrupted planetesimals during collisions, along with the appearance of secondary shock waves containing condensed particles and the transport of gas containing condensed particles subjected to impact heating, subsequently undergoes non-uniform mixing with the plume's edge and interior. Many objects in these regions may have been physically destroyed and vaporized completely, then reformed through recondensation and reaccretion.

5 Conclusion

The SG 013 meteorite, as a representative of the CBa type of carbonaceous chondrite, sheds light on the extreme conditions and dynamic evolution of material differentiation in the early Solar System through its complex spotted and metallic silicate chondrules. In-depth analysis using Electron Backscatter Diffraction (EBSD) technology on olivine reveals that this meteorite has undergone high-temperature rapid melting and cooling, as well as localized impact or heating events, resulting in zonal and spot-textured structures. These structures indicate variations in temperature gradients and strain rates within the impact plume, influencing mineral deformation and recrystallization mechanisms. The formation of metallic silicate chondrules is associated with the compaction of olivine grains, while recrystallization in L2 lithologies is attributed to thermal shock metamorphism.

The microstructural characteristics of olivine not only reflect the thermodynamic and kinetic processes within the plume but also provide crucial insights into the history of the early Solar System. Chondrites are formed by the ejection of melt droplets into the impact plume, followed by gas-melt interactions. The metal-silicate globule brought in by the impact plume edge originated from the accretion breccia of the impact debris. They are the result of uniaxial compression under the low temperature and fast strain rate in the Plume interior, and the strong points are very dense. However, under the condition of higher temperature and lower strain rate at the edge of the plume, the girdle develops very dense.

Acknowledgements This work is supported by Strategic Priority Research Program (B) of Chinese Academy of Science (Grant No. XDB 41000000).

Author contributions R. Li processed the samples, collected the data and wrote up the first draft; C.-H., Li designed the project; W. Chen provided help on instrumentation. All authors contribute to the data interpretation and improvement of the manuscript.

Funding Chinese Academy of Science,XDB 41000000,Chunhui Li

Declarations

Conflicts of interest The authors have no conflicts of interest to declare.

References

Bollard J, Connelly JN, Bizzarro M (2015) Pb-Pb dating of individual chondrules from the CB_a chondrite Gujba: Assessment of the impact plume formation model. Meteorit Planet Sci 50(7):1197–1216. https://doi.org/10.1111/maps.12461

Campbell AJ, Humayun M, Weisberg MK (2002) Siderophile element constraints on the formation of metal in the metal-rich chondrites Bencubbin, Weatherford, and Gujba. Geochim Cosmochim Acta 66(4):647–660. https://doi.org/10.1016/S0016-7037(01)00794-3

Carter PJ, Stewart ST (2020) Colliding in the shadows of giants: planetesimal collisions during the growth and migration of gas giants. Planet Sci J 1(2):45. https://doi.org/10.3847/psj/abaecc

Connolly HC, Hewins RH (1995) Chondrules as products of dust collisions with totally molten droplets within a dust-rich nebular environment: an experimental investigation. Geochim Cosmochim Acta 59(15):3231–3246. https://doi.org/10.1016/0016-7037(95)00207-G

Gooding JL, Keil K (1981) Relative abundances of chondrule primary textural types in ordinary chondrites and their bearing on conditions of chondrule formation. Meteoritics 16(1):17–43. https://doi.org/10.1111/j.1945-5100.1981.tb00183.x

Hasegawa Y, Wakita S, Matsumoto Y, Oshino S (2016) Chondrule formation *via* impact jetting triggered by planetary accretion. Astrophys J 816(1):8. https://doi.org/10.3847/0004-637x/816/1/8

Hewins RH, Condie C, Morris M, Richardson MA, Ouellette N, Metcalf M (2018) Thermal history of CB_b chondrules and cooling rate distributions of ejecta plumes. Astrophys J Lett 855(2):L17. https://doi.org/10.3847/2041-8213/aab15b

Ivanova MA, Lorenz CA, Humayun M, Yang SY, Ma C, Teplyakova SN, Franchi IA, Korochantsev AV (2022) Sierra gorda 013: unusual CBa-like chondrite. Meteorit Planet Sci 57(3):657–682. https://doi.org/10.1111/maps.13786

Ivanova MA, Somsikova AV, Lorenz CA, Kostitsyn YA (2023) Study of Rb-Sr and Sm-Nd isotopic systems in chondrules of the sierra gorda 009 and 013 chondrites and possible mechanisms of their disturbance. Geochem Int 61(6):562–571. https://doi.org/10.1134/S0016702923060058

Kallemeyn GW, Boynton WV, Willis J, Wasson JT (1978) Formation of the bencubbin polymict meteoritic breccia. Geochim Cosmochim Acta 42(5):507–515. https://doi.org/10.1016/0016-7037(78)90200-4

Krot AN, Nagashima K, Ivanova MA, Humayun M, Libourel G, Johnson BC, Cashion MD, Bizzarro M (2022a) Oxygen isotopic compositions of minerals in chondritic and achondritic lithologies of the CB carbonaceous chondrite Sierra Gorda 013. LPI Contributions 2695:6100

Krot AN, Petaev MI, Nagashima K, Dobrică E, Johnson BC, Cashion MD (2022b) Impact plume-formed and protoplanetary disk high-temperature components in CB and CH metal-rich carbonaceous chondrites. Meteorit Planet Sci 57(2):352–380. https://doi.org/10.1111/maps.13717

Krot AN, Nagashima K, Ivanova MA, Lauretta D, Libourel G, Johnson BC, Brenker FE, Hoffman V, Bizzarro M (2023) Mineralogy, petrology, and oxygen isotopic compositions of chondritic and achondritic lithologies in the anomalous CB carbonaceous chondrites Sierra Gorda 013 and Fountain Hills. Meteorit Planet Sci. https://doi.org/10.1111/maps.14072

Lofgren G (1989) Dynamic cyrstallization of chondrule melts of porphyritic olivine composition: textures experimental and natural. Geochim Cosmochim Acta 53(2):461–470. https://doi.org/10.1016/0016-7037(89)90397-9

Lofgren G, Russell WJ (1986) Dynamic crystallization of chondrule melts of porphyritic and radial pyroxene composition. Geochim Cosmochim Acta 50(8):1715–1726. https://doi.org/10.1016/0016-7037(86)90133-X

Lorenz CA, Ivanova MA, Zinovieva NG, Ryazantsev KM, Korochantsev AV (2023) Heterogenity of planetesimal collisional plume probed by glass inclusions in metal globules of Sierra Gorda 013, an unusual CBa-like chondrite. Meteorit Planet Sci 58(2):241–258. https://doi.org/10.1111/maps.13951

Meibom A, Petaev MI, Krot AN, Wood JA, Keil K (1999) Primitive FeNi metal grains in CH carbonaceous chondrites formed by condensation from a gas of solar composition. J Geophys Res 104(E9):22053–22059. https://doi.org/10.1029/1999je001052

Meibom A, Righter K, Chabot N, Dehn G, Antignano A, McCoy TJ, Krot AN, Zolensky ME, Petaev MI, Keil K (2005) Shock melts in QUE 94411, hammadah al Hamra 237, and bencubbin: remains of the missing matrix? Meteorit Planet Sci 40(9–10):1377–1391. https://doi.org/10.1111/j.1945-5100.2005.tb00408.x

Oulton J, Humayun M, Fedkin A, Grossman L (2016) Chemical evidence for differentiation, evaporation and recondensation from silicate clasts in Gujba. Geochim Cosmochim Acta 177:254–274. https://doi.org/10.1016/j.gca.2016.01.008

Rubin AE, Kallemeyn GW, Wasson JT, Clayton RN, Mayeda TK, Grady M, Verchovsky AB, Eugster O, Lorenzetti S (2003) Formation of metal and silicate globules in Gujba: A new Bencubbin-like meteorite fall. Geochim Cosmochim Acta 67(17):3283–3298.

Sanders IS, Taylor GJ (2005) Implications of ^{26}Al in nebular dust: Formation of chondrules by disruption of molten planetesimals. In: (Krot AN, Scott ERD, Reipurth B eds.) ASP Conference Series: Chondrites and the protoplanetary disk. 341:915.

Scott ER (2007) Chondrites and the protoplanetary disk. Annu Rev Earth Planet Sci 35(1):577–620. https://doi.org/10.1146/annurev.earth.35.031306.140100

Stewart ST, Carter PJ, Davies EJ, Lock S, Kraus R, Root S, Petaev MI, Jacobsen S (2019) Collapsing impact vapor plume model for chondrule and chondrite formation. 50th Annual Lunar Planet Sci Conf. 50: 1251

Weisberg MK, Prinz M, Clayton RN, Mayeda TK, Sugiura N, Zashu S, Ebihara M (2001) A new metal-rich chondrite grouplet. Meteorit Planet Sci 36(3):401–418. https://doi.org/10.1111/j.1945-5100.2001.tb01882.x

Weyrauch M (2018) The origin of metal and chondrules in CH and CB chondrites: Evidence from Fe, Ni, and Si isotopes and trace element compositions (PhD Dissertation). Uni Hannover, Germany

Wlotzka F (1993) A weathering scale for the ordinary chondrites. Meteoritics 28(3):460